# Microwave Irradiation Effects on Structural and Optical Investigations of Nanostructured $Ge_{25}Se_{75}$ Glassy Films

M. Rashad[a,b,*], A. Mossad Ali[c], H.H. Somaily[c], H. Algarnl[c], D. Hamad[a], A.A. Hendi[d] and M.M. Hafiz[a]

[a] *Physics Department, Faculty of Science, Assiut University, Assiut 71516, Egypt*
[b] *Department of Physics, and Nanotechnology Research Unit, Faculty of Science, University of Tabuk, Tabuk 71491, Saudi Arabia*
[c] *Physics Department, Faculty of Science, King Khalid University, Abha, Saudi Arabia*
[d] *Department of Physics, Faculty of Science, University of Jeddah, P.O Box 80327, Jeddah, 21589 Saudi Arabia*

Received: 31.01.2020 & Accepted: 22.04.2020

Doi: 10.12693/APhysPolA.138.434 *e-mail: mohamed.ahemed24@science.au.edu.eg

$Ge_{25}Se_{75}$ binary glass is prepared using melt-quenching technique. Thin films of 250 nm $Ge_{25}Se_{75}$ are thus evaporated using thermal evaporation method on a cleaned glass substrate. Energy dispersive X-ray analysis confirmed the starting percentage of the element. The effect of microwave irradiation on $Ge_{25}Se_{75}$ thin film with different illumination times (0–90 min) is studied. As confirmed by X-ray diffraction and scanning electron microscopy measurements, the nature of the as-prepared $Ge_{25}Se_{75}$ thin films appears to be amorphous. The type of optical transition has been demonstrated to be allowed indirect transitions. Moreover, the rest of the optical parameters have changed as a result of the microwave irradiation. It can be observed that, for $Ge_{25}Se_{75}$ thin films, the optical band gap increases as the illumination time increases. In terms of bond adjustments and changes in these films' microstructure, this post-light increment in the band gap was decoded. Furthermore, while increasing the illumination time of microwave irradiation, the dispersion parameters of $Ge_{25}Se_{75}$ films were diminished.

topics: Ge–Se, thin films, microwave irradiation, structural investigations, optical properties

## 1. Introduction

Chalcogenide glasses consist of group VI components (S, Se, and Te) in the periodic table. These glasses can be regarded to be semiconductor materials [1]. Recently, these glasses are gaining an increasing interest owing to their potential applications in solid-state electronic and optical devices, such as phase-change optical recording, optical imaging, memory exchanging, nondirect optics, and photolithography [2]. Ge–Se is a common chalcogenide semiconductor, which can be effectively arranged either in glass or in crystalline structure. Recently, numerous researches on Ge–Se glass have been conducted to examine rigidity percolation and short and transitional range order of the structure [3–5]. The microwave energy has become an intriguing branch for studying [6–8]. The developing interest during the past decade is basically due to the plausibility of assembly, cost reduction through energy reserve, shorter preparation times, and improved product consistency and yields. For the most part, microwave processing differs in that the heat is created within the material rather than in an external heating source, a reality that is responsible for the one of a kind microstructure and consistency. Microwave processing has been employed in annealing ferroelectric films [9]. Microwave irradiation has shown rapid development in its application in material science owing to its unique response impacts, for example, quick volumetric heating and the ensuing sensational increment in response rates. This paper presents the effect of microwave irradiation on the $Ge_{25}Se_{75}$ thin films with different illumination times (0–90 min). X-ray diffraction (XRD) has been utilized to study the structural nature. Optical reflection and transmission spectra of $Ge_{25}Se_{75}$ chalcogenide thin films have been obtained in the range 200–2500 nm at room temperature. The optical parameters have changed with the microwave irradiation.

## 2. Experimental techniques

$Ge_{25}Se_{75}$ bulk chalcogenide glasses were set up by the melt-quenching system. Materials (99.999% pure) were weighted by their atomic rates and were fixed in an evacuated silica tube, which was heated

at 1100 °C for 15 h. The tube was shocked at maximum temperature in order to make the solution homogeneous; this took place in ice water. Films were prepared using thermal evaporation at vacuum in $10^{-5}$ Torr by an Edwards E-306 coating unit. The evaporation rates and film thickness were restricted using a quartz screen, Edwards model FTMS. The chemical composition of the samples was determined using the standard energy dispersive X-ray (EDX) analysis technique, JEOL JSM-T200 type, Japan.

X-ray examination of the as-prepared films was carried out using Philips Diffractometer 1710 with Ni with $CuK_\alpha$ source ($\lambda = 0.154$ nm). A microwave with 650 W power (Sanle General Electric Corp. Nanjing, China) was utilized for different illumination times (0–90 min).

The scanning electron microscopy (SEM) images were recorded on a JEOL JEM200CX scanning electron instrument.

Transmittance $T(\lambda)$ and reflectance $R(\lambda)$ were recorded at room temperature using a double beam spectrophotometer (Shimadzu UV-2101).

## 3. Results and discussions

### 3.1. Structural properties

EDX spectra of $Ge_{25}Se_{75}$ films show the element percentage in Fig. 1. The percentage of these elements nearly agrees with the starting bulk material. Figure 2 shows the XRD patterns for the as-prepared $Ge_{25}Se_{75}$ thin films at different microwave illumination times (0–90 min). In Fig. 2a the amorphous nature of the as-prepared $Ge_{25}Se_{75}$ thin film is illustrated. Figure 2b and 2c reveals that the amorphous nature still exists in time, but there were some peaks after the 45 min illumination time. Additionally, some peaks appeared after the 90 min illumination time. These peaks suggested that there are certain bonds appearing, being Ge–Se bonds, indicating that the microwave illumination time had an impact on the structural figure of these films.

The surface morphology of the studied films was analyzed before and after illumination time of 90 min. Figure 3 displays the SEM images for

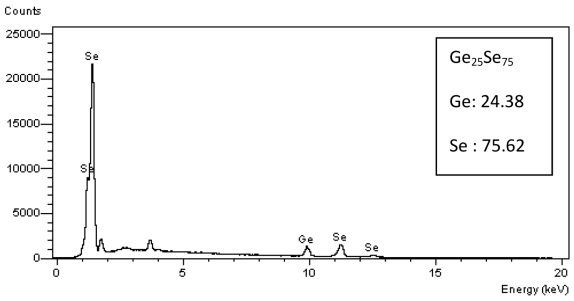


Fig. 1. EDX spectra of as prepared $Ge_{25}Se_{75}$ thin films.

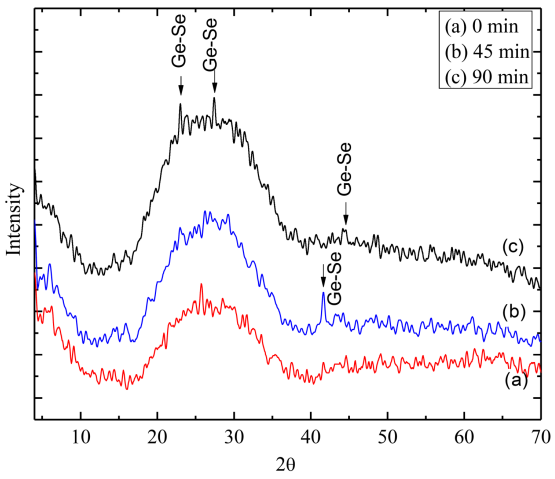


Fig. 2. XRD patterns for as-prepared $Ge_{25}Se_{75}$ thin films and after microwave irradiation at different illumination time.

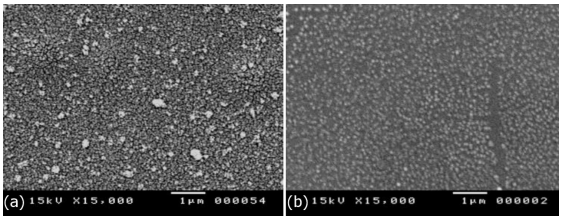


Fig. 3. SEM images for as-prepared $Ge_{25}Se_{75}$ thin films onto glass substrate (a) and after microwave irradiation time of 90 min (b).

the as-prepared $Ge_{25}Se_{75}$ thin films onto glass substrate and after microwave irradiation time of 90 min. It is observed that there are small crystallites dispersed over the surface of an amorphous matrix as shown in Fig. 3a. These crystallites were smaller in size after microwave irradiation time of 90 min as one can see in Fig. 3b.

### 3.2. Optical investigations

#### *3.2.1. Absorption coefficient*

At different induced microwave irradiation times (0–90 min), the transmittance $T$ and reflectance $R$ were captured for 250 nm $Ge_{25}Se_{75}$ films and shown in Fig. 4. It is found that $T$ increases with $R$ decreasing as time increases. In addition, the transmittance edge is shifted towards a lower wavelength indicated that the energy gap will increase as the time increases.

Therefore, the absorption coefficient ($\alpha$) should be calculated using both values of $T$ and $R$ according to the following equation [10]:

$$\alpha = \frac{1}{d} \ln \left( \frac{(1-R)^2}{2T} + \sqrt{R^2 + \frac{(1-R)^4}{4T^2}} \right), \quad (1)$$

where $d$ [cm] is the film thickness.

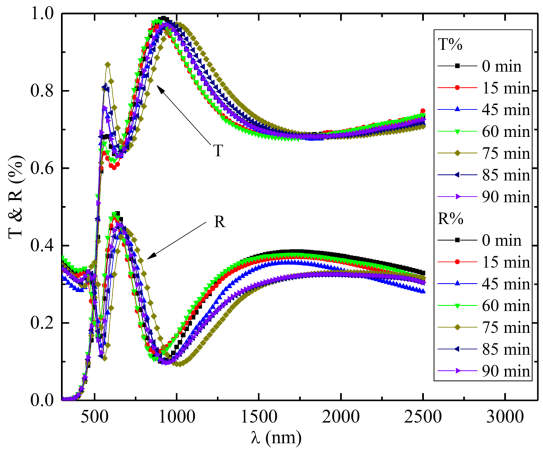


Fig. 4. Transmittance $T$ and reflectance $R$ for $Ge_{25}Se_{75}$ film with different illumination time (0–90 min).

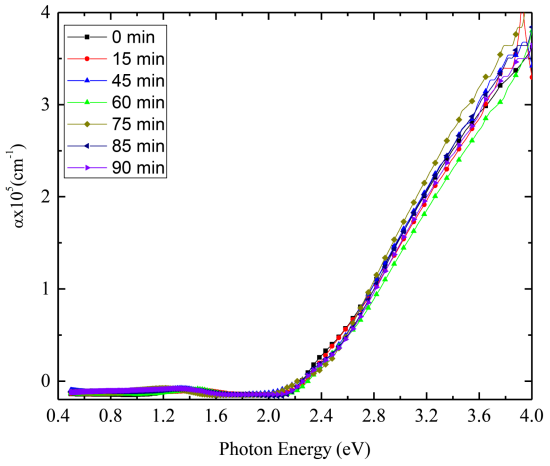


Fig. 5. The absorption coefficient vs. photon energy of $Ge_{25}Se_{75}$ film with different illumination time.

Figure 5 shows the dependence of $\alpha$ on the incident photon energy $h\nu$ for the as-prepared $Ge_{25}Se_{75}$ thin films illuminated at different times. A decreasing behavior of $\alpha$ with induced time is observed. To understand these behaviors in more detail, the $\alpha$ values less than $10^4$ cm$^{-1}$ are called the Urbach tail. In this range, $\alpha$ is depending exponentially on $h\nu$ which is captured with the formula [11]:

$$\alpha(\nu) = \alpha_0 \exp(h\nu/E_e), \tag{2}$$

where $\nu$ is radiation frequency, $E_e$ is a localized states tails' width.

Figure 6 shows the dependence of $\ln(\alpha)$ on the incident photon energy $h\nu$ for the as-deposited glass $Ge_{25}Se_{75}$ illuminated at different times. The values of the width of the tails of localized states are listed in Table I.

In the range when $\alpha > 10^4$ cm$^{-1}$, one can express its dependence on $h\nu$ as [12, 13]:

$$\alpha(h\nu) = A(h\nu - E_g)^m, \tag{3}$$

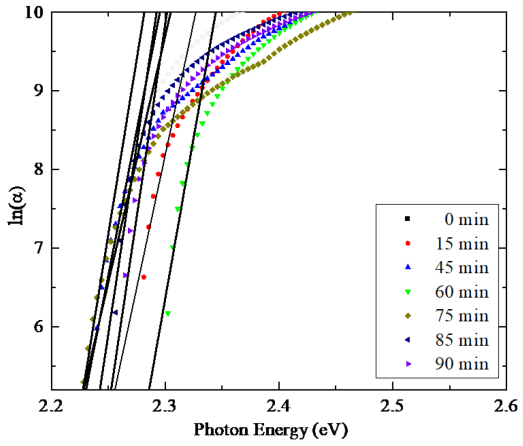


Fig. 6. $\ln\alpha$ vs. photon energy of $Ge_{25}Se_{75}$ film with different illumination time.

TABLE I

Some optical parameters vs. different irradiation time of $Ge_{25}Se_{75}$ thin films.

| Illumination time [min] | $E_g^{\text{in}}$ [eV] | $E_e$ [meV] | $\epsilon_L$ | $N/m*$ [$10^{56}$ kg$^{-1}$ m$^{-3}$] |
|---|---|---|---|---|
| 0 | 2 | 16 | 23 | 6.2 |
| 15 | 2.05 | 15 | 22 | 6.2 |
| 45 | 2.07 | 14 | 20 | 5.9 |
| 60 | 2.1 | 12 | 21 | 5.3 |
| 75 | 2.11 | 11 | 16 | 2.2 |
| 85 | 2.12 | 10.3 | 15 | 1.6 |
| 90 | 2.13 | 10.2 | 15 | 1.64 |

where $E_g$ is an optical band gap, and $m$ is a power indicated in the transition process. If $m = 2$, one has an indirect allowed transition. Otherwise, if $m = 1/2$, a direct allowed transition occurs. Figure 7 explains the dependence of $\sqrt{\alpha h\nu}$ on the incident photon energy $h\nu$ for the as-deposited $Ge_{25}Se_{75}$ illuminated at different times. Using a linear regression the straight line is drawn to better estimates behaviour of the plotted points. Thus, the values of $m$ are $2 \pm 0.05$. When the value of $m$ is closed to 2, this indicates that the electronic transition responsible for the photon absorption is a nondirect process. Figure 6 illustrates linear plot of $\sqrt{\alpha h\nu}$ versus photon energy $h\nu$ of the two films with different film thickness. The intercept of the straight line with the photon energy axis at $\sqrt{\alpha h\nu} = 0$ gives the optical band gap $E_g$. The results collected for $Ge_{25}Se_{75}$ in Table I indicate that $E_g$ values increase for increasing values of illumination time.

In case of the optical band gap, it was shifted slightly from 2 eV to 2.13 eV due to irradiation. Microwave irradiation leads to the breaking of bonds and formation of new ones, in turn resulting in the decrease of dangling bonds and defects and trapping generated carriers. This triggers the decrease

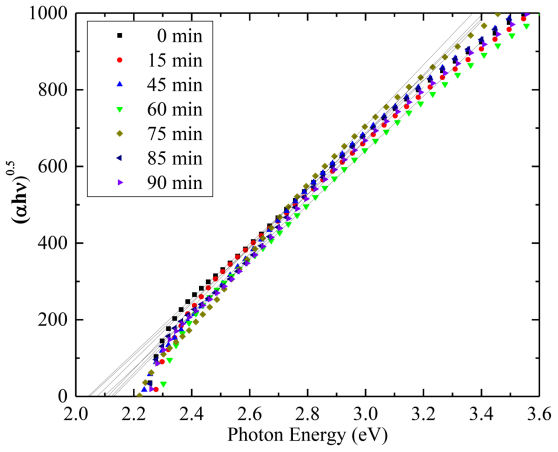


Fig. 7. $(\alpha h\nu)^{0.5}$ vs. photon energy of $Ge_{25}Se_{75}$ film with different illumination time.

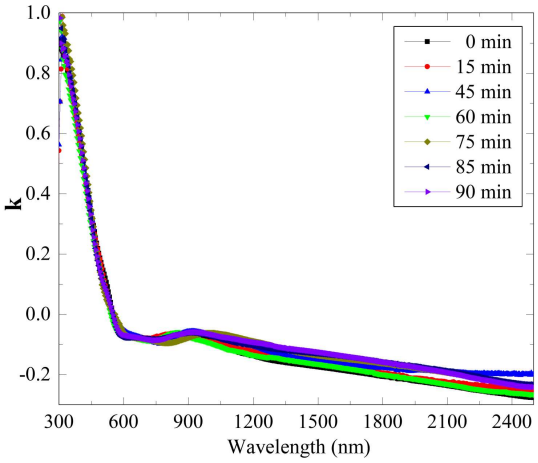


Fig. 8. Extinction coefficient $k$ vs. wavelength $\lambda$ of $Ge_{25}Se_{75}$ film with different illumination time.

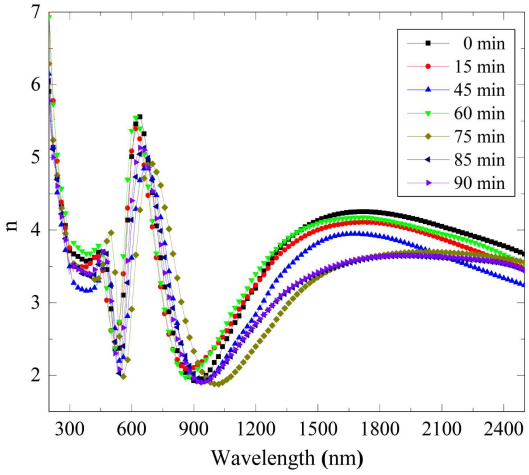


Fig. 9. Refractive index $n$ vs. wavelength $\lambda$ of $Ge_{25}Se_{75}$ film with different illumination time.

in band tail width, then the energy gap expands as the homopolar bond decreases [14]. These homopolar bonds, such as Se–Se bonds defects, are related to localized states on the band structure. Due to annealing, these unsaturated defects are gradually annealed out, and thus the optical band gap increases. Moreover, the annealing sources, such as thermal, light, or microwave annealing, cause a decrease in homopolar bonds, indicating the increase of the optical band gap [15].

The extinction coefficient $k$ could be represented in the form [16, 17]:

$$a = \frac{4\pi k}{\lambda}. \tag{4}$$

The dependence of $k$ on $\lambda$ is observed in Fig. 7. It is observed that $k$ values for the as-deposited $Ge_{25}Se_{75}$ films are less (or decreased) than the irradiated $Ge_{25}Se_{75}$ films. This can be attributed to the reason mentioned previously — to the absorption coefficient that has the same behavior.

### *3.2.2. Dispersion analysis*

Refractive index is considered to be one of the key properties of an optical material, since it is closely associated with the electronic polarizability of ions and the local field inside materials. In some applications, especially in optical devices, the assessment of the refractive file of optical material is important.

The refractive index $n$ can be calculated using [18, 19]:

$$n = \left(\frac{1+R}{1-R}\right) + \sqrt{\frac{4R}{(1-R)^2} - k^2}. \tag{5}$$

Figure 8 displays the refractive index $n$ as a function of wavelength for $Ge_{25}Se_{75}$ films with different illumination times. It is clear from Fig. 9 that there are two regions of refractive index $n$ spectrum for the irradiated film. The first region occurs at $\lambda = 1000$–$1700$ nm, and the second region starts where $\lambda$ exceeds 1700 nm. The refractive index $n$ increases in the first region, resulting from the electronic transitions of the valence band and the impurities (or an increase of the compactness of the films) and the transitions of energy bands. These values are reduced with increase in wavelengths. In the second region of the spectrum, the variation of refractive index $n$ with wavelengths becomes slightly decreased and its values are very close at cut-off wavelength. On the other hand, a deviation from the linear behavior is seen at a longer wavelength, which is attributable to the negative contribution of the lattice vibration [20]. Real and imaginary dielectric constants for $Ge_{25}Se_{75}$ at different illumination times can be calculated using the following equations [21, 22]:

$$\epsilon_r = n^2 - k^2, \tag{6}$$

$$\epsilon_i = 2nk. \tag{7}$$

Figures 10 and 11 show the variation of real and imaginary dielectric constants for $Ge_{25}Se_{75}$ films at different illumination times. The variation of $\varepsilon_i$ and nearly ignoring $n$ are because of the ignored values of $k^2$ compared to $n^2$. On the other hand,

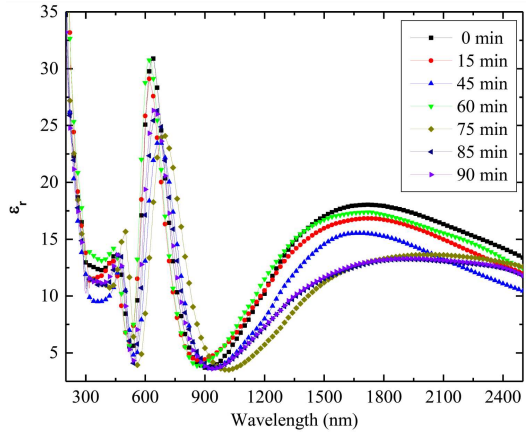


Fig. 10. Real part of dielectric constant $\varepsilon_r$ vs. wavelength $\lambda$ of $Ge_{25}Se_{75}$ film with different illumination time.

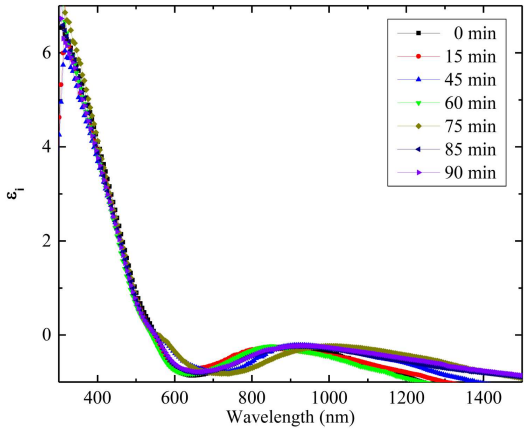


Fig. 11. As in Fig. 10, but for imaginary part.

$\varepsilon_r$ mainly depends on the value of $k$, illustrating the radiation absorption by free carriers [24]. It is observed that $\varepsilon_i$ increases and decreases with irradiation, and this is attributed to the same reason mentioned previously for the refractive index, while $\varepsilon_r$ increases with increase in the irradiation, and this is due to the similar interpretation discussed previously for the extinction coefficient. Single oscillator model [17, 18] is used for analyzing the data of refractive index in the normal dispersion area, describing the dielectric response for the transition below the band gap.

High-frequency dielectric constant is very important because of its contribution of free carriers and dispersion lattice vibration modes. Therefore, it could be determined by analyzing the data of refractive index. The dependence of the real dielectric constant ($\varepsilon_r = n^2$) on $\lambda$ in the normal dispersion area could be given by the following [18, 23]:

$$n^2 = \epsilon_L - \frac{e^2}{4\pi^2 c^2 \epsilon_0}\frac{N}{m*}\lambda^2 \qquad (8)$$

where $\varepsilon_L$ is the lattice dielectric constant, $e$ is electronic charge, $\varepsilon_0$ is permittivity of free space, $N/m^*$ is the ratio of carrier concentration to the effective mass.

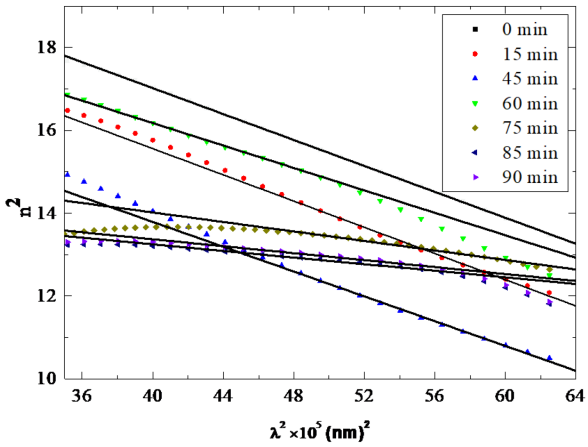


Fig. 12. $n^2$ vs. $\lambda^2$ of $Ge_{25}Se_{75}$ film with different illumination time.

The dependence of $n^2$ on $\lambda^2$ appears in Fig. 12 and it is seen that the reliance of $n^2$ on $\lambda^2$ is linear at longer wavelengths. Extrapolating the direct parts of this reliance to zero wavelengths gives the estimations of $\varepsilon_L$. From the slope of the linear parts, one could obtained the values of $N/m^*$ which were listed in Table I. The values of $N/m^*$ (related to the internal microstructure) diminish with expanding microwave-induced time. Such behavior is interpreted as the creation of additional trapping carriers, uniting with the original carriers in the films.

## 4. Conclusion

Nanostructured $Ge_{25}Se_{75}$ films were set up by thermal evaporation procedure. XRD studies show that, upon microwave-induced time, an adjustment in the microstructure of the films happens due to their adaptable structure. The absorption coefficients of these films, upon illumination, are of the order for $10^5$ cm$^{-1}$. As a consequence, such materials may have an industrial application as optical recording media. The $Ge_{25}Se_{75}$ band gap has an allowed indirect transition of increments of 2–2.13 as the microwave-induced increments 0–90 min. The impact of microwave induction should be associated with bond adjustments and changes in the microstructure of these films. The refractive index diminishes with the expansion of the microwave-induced time. Investigation of the experimental results highlights that the dispersion parameters of $Ge_{25}Se_{75}$ at various induced times diminished with increments in those times.

## Acknowledgments

The authors extend their appreciation to the Deanship of Scientific Research at King Khalid University for funding this work through research groups program under grant no. R.G.P. 2/33/40.

## References


[1] R. Kumar, P. Sharma, V.S. Rangra, *J. Therm. Anal. Calorim.* **109**, 177 (2012).

[2] M. Rashad, R. Amin, M.M. Hafiz, *Chalcog. Lett.* **12**, 441 (2015).

[3] M. Rashad, A.A.A. Darwish, A.A.S. Farha Said, A.A. Hendi, M.M. Hafiz, *Chin. J. Phys.* **56**, 212 (2018).

[4] M.F. Thorpe,*J. Non-Cryst. Solids* **182**, 355 (1995).

[5] C. Massobrio, A. Pasquarello, *Phys. Rev. B* **77**, 144207 (2008).

[6] W.H. Sutton, *Am. Ceram. Soc. Bull.* **68**, 376 (1989).

[7] R. Roy, D. Agrawal, J. Cheng, S. Gedevanishvili, *Nature 399*, 668 (1999).

[8] Z. Cao, Z. Wang, N. Yoshikawa, S. Taniguchi, *J. Phys. D Appl. Phys.* **41**, 092003 (2008).

[9] A. Bhaskar, T. Hsu Chang, H. Yi Chang, S. Yu Cheng, *Appl. Surf. Sci.* **255**, 3795 (2009).

[10] A.A. Hendi, M. Rashad, *Physica B Condens. Matter* **538**, 185 (2018).

[11] A.A. El-Fadl, G.A. Mohamad, A.B.A. El-Moiz, M. Rashad, *Physica B Condens. Matter* **366**, 44 (2005).

[12] S.I. Qashou, M. Rashad, A.A.A. Darwish, T.A. Hanafy, *Opt. Quant. Electron.* **49**, 240 (2017).

[13] M.M. El-Nahass, A.A. Atta, H.E.A. El-Sayed, E.F.M. El-Zaidia, *Appl. Surf. Sci.* **254**, 2458 (2007).

[14] B. Mukta, B. Sunita, N. Ramakanta, *RSC Adv.* **7**, 18428 (2017).

[15] W. Li, S. Seal, C. Rivero et al., *J. Appl. Phys.* **98**, 053503 (2005).

[16] P. Nemec, J. Jedelsky, M. Frumar, M. Munzar, M. Jelinek, J. Lanccok, *J. Non-Cryst. Solids* **326-327**, 53 (2003).

[17] A.H. Moharram, S.A. Mansour, M.A. Hussein, M. Rashad, *J. Nanomater.* **2014**, 20 (2014).

[18] M. Rashad, A.A.A. Darwish, A.A. Attia, *J. Non-Cryst. Solids* **470**, 1 (2017).

[19] M.M. El-Nahass, H.S. Soliman, N. El Kadry, A.Y. Morsy, S. Yaghmour, *J. Mater. Sci. Lett.* **7**, 1050 (1988).

[20] R.A. Grenier, *Electronic Energy Series*, McGraw-Hill, 1961.

[21] M. Rashad, A.A.A. Darwish, *Mater. Res. Express* **5**, 026402 (2018).

[22] P. Burrows, S. Forrest, *J. Appl. Phys.* **79**, 7991 (1996).

[23] M.M. El-Nahass, Z. El-Gohary, H.S. Soliman, *Opt. Laser Technol.* **35**, 523 (2003).